# ГЕОІНФОРМАТИКА



**UDC 528.97:004.9:551.583**
**DOI: http://doi.org/10.17721/1728-2713.112.14**

**Serhii MARHES[1], PhD Student**
**ORCID ID: 0009-0004-2942-9406**
**e-mail: sergemarhes@gmail.com**

**Vasyl HUDAK[2], PhD Student,**
**ORCID ID: 0009-0002-7333-0409**
**e-mail: gudak_vasyl@knu.ua**

**Vitaliy ZATSERKOVNYI[2], DSc (Engin.), Prof.**
**ORCID ID: 0009-0003-5187-6125**
**e-mail: vitalii.zatserkovnyi@knu.ua**

**Volodymyr FILIPOVYCH[1], PhD (Geol.), Senior Researcher**
**ORCID ID: 0000-0002-9404-8122**
**e-mail: vefilin2000@gmail.com**

**Mauro DE DONATIS[3], PhD (Geol.), Assoc. Prof.**
**ORCID ID: 0000-0002-9721-1095**
**e-mail: mauro.dedonatis@uniurb.it**

**[1]State Institution "Scientific Centre for Aerospace Research of the Earth of the Institute of Geological Sciences of the National Academy of Sciences of Ukraine", Kyiv, Ukraine**
**[2]Taras Shevchenko National University of Kyiv, Kyiv, Ukraine**
**[3]University of Urbino Carlo Bo, Urbino, Italy**

# DETECTION OF SOIL DEGRADATION PROCESSES IN RIVER BASINS USING SATELLITE INDICES AND A CUSTOM QGIS PLUGIN

(*Представлено членом редакційної колегії д-ром с.-г. наук, проф. Оксаною ТОНХОЮ*)

**Background.** *This study addresses the challenge of identifying and assessing soil degradation risks in river basins, which significantly impact the ecological state of territories. Special emphasis is placed on enhancing the efficiency of spatial analysis through the use of an advanced QGIS plugin developed by the authors.*

**Methods.** *The software tool was implemented using the OSGeo Python package and integrates algorithms for weighted overlay and semi-automated vectorization of results. It is designed as an internal function set that requires no additional installations. The plugin's functionality includes satellite data processing, automated detection of anomalous zones, and the construction of a generalized correspondence table linking spectral indices to specific forms of degradation. The analysis employed multi-decadal Landsat imagery (1985–2025) together with Sentinel-2 data (2025), processed within the QGIS environment. Testing was conducted in two contrasting study areas – the Dnipro and Supii river basins – characterized by markedly different levels of anthropogenic pressure.*

**Results.** *The analysis revealed clear patterns of soil degradation processes, including vegetation decline, salinization, waterlogging, drought manifestations, and erosion. The use of the generalized spectral index table optimized the interpretation of satellite imagery, enhancing the reliability of classifying degradation types. The plugin demonstrated high effectiveness in integrating index-based analysis with spatial modeling, thereby enabling comprehensive evaluation of basin systems.*

**Conclusions.** *The enhanced tool proved its practical applicability for ecological monitoring and decision support. A key innovation lies in the integration of semi-automated remote sensing interpretation with multi-level index classification, enabling both rapid anomaly detection and detailed spatio-temporal assessment of degradation dynamics. Prospective directions for development include the incorporation of machine learning algorithms for automated classification, the use of Big Data processing and parallel computing to ensure scalability, and integration with cloud-based platforms such as Google Earth Engine to provide real-time access to updated data streams. Collectively, these advancements lay the methodological foundation for developing a universal system to forecast and mitigate degradation processes in river basins.*

**Keywords:** *GIS, monitoring, exogenic geological processes, soil degradation, satellite imagery, automated detection, geospatial zones, QGIS plugin, geodynamic anomalies, spatial analysis.*

## Background

Urbanization is one of the primary drivers of environmental transformation under conditions of increasing anthropogenic pressure. The expansion of metropolitan areas, infrastructure development, industrialization, and changes in land use substantially modify hydrological regimes, soil cover, and landscape structures. Urban territories are characterized by fragmentation of natural ecosystems, soil compaction, biodiversity loss, and elevated levels of environmental pollution (Kravchenko, 2023).

At the same time, geoecological changes are shaped not only by anthropogenic impacts but also by natural (exogenous) processes such as erosion, suffusion, landslides, flooding, and climatic variability, all of which strongly influence landscape morphology and soil conditions (Shekhunova, & Kril, 2022). The interplay between natural and anthropogenic drivers complicates the attribution of degradation sources and underscores the need for comprehensive monitoring (Higginbottom, & Symeonakis, 2014; Keesstra et al., 2016).



ISSN 1728-3817

Globally, soil degradation ranks among the most pressing ecological challenges, especially in regions with arid climates, intensive land exploitation, and unsustainable agricultural practices (Kruglov, Hudak, & Kruhlov, 2025). Its manifestations include desertification and overgrazing in Sub-Saharan Africa, deforestation in the Amazon Basin, salinization and water erosion in South Asia, wind erosion in northern China, humus depletion and surface erosion in Southern Europe, and salinization coupled with aeolian deflation in Australia (Bouza et al., 2016; Yirdaw, Tigabu, & Monge, 2017).

In Ukraine, the drivers of soil degradation differ across urban and rural contexts. In major cities such as Kyiv, degradation is mainly associated with urbanization and anthropogenic stress. According to Korohoda, Kovtoniuk, and Halahan (2023), heavy metal contamination (Pb, Cd, Zn) is widespread near industrial facilities and highways, reducing soil fertility and vegetation health. Recreational overuse of green areas additionally contributes to soil compaction, lower permeability, and loss of organic matter, thereby accelerating erosion.

In rural areas, degradation is more closely related to water and wind erosion, salinization, and acidification. Menshov and Kruglov (2023) report that water erosion affects nearly 40 % of agricultural land, resulting in severe losses of fertile topsoil. Wind erosion in steppe zones amplifies soil deflation, while excessive application of mineral fertilizers and insufficient crop rotation exacerbate acidification, undermining soil fertility and agronomic performance.

These processes are especially destructive within river basin systems, which act as accumulators of direct and indirect anthropogenic pressures. Riparian zones – transition zones between terrestrial and aquatic ecosystems – are particularly vulnerable (Ivanik et al., 2022). They are prone to erosion, salinization, hydrological alterations, flooding, and aeolian activity. Under urbanization, riparian systems frequently lose ecological resilience, leading to soil degradation and destabilization of local ecosystems (Nath et al., 2023).

Against this background, remote sensing (RS) and geographic information systems (GIS) have become indispensable tools for high-precision monitoring of soil cover dynamics (Xie, Xiao, & Ashraf, 2020). Integration of Earth observation datasets (e.g., Sentinel-2) with basin-scale approaches provides objective insight into the scale and dynamics of degradation processes (Adgo, Teshome, & Mati, 2013).

This study introduces the application of an upgraded GIS plugin, developed by the authors for QGIS (Hudak et al., 2025; Marhes, & Hudak, 2025), designed to support geoecological analysis of riparian zones. The plugin enables automated identification of anomalous areas in satellite imagery – defined as locations where spectral indicators deviate statistically from background environmental conditions. Such anomalies include elevated or reduced index values (e.g., NDWI, TIR, InSAR), which capture features such as thermal anomalies, moisture deficits, or vertical ground displacements (Hudak, Kril, & Zatserkovnyi, 2025).

For the case study, two contrasting areas were selected:

• the urbanized banks of the Dnipro River within Kyiv, characterized by high anthropogenic pressure, dense construction, intensive recreational activity, and substantial transport and technogenic impacts (Filipovych, Lischenko, & Marhes, 2025; Kril, Cherevko, & Shekhunova, 2024);

• the riparian area of the Supii River, a left tributary of the Dnipro, situated within predominantly agricultural landscapes with limited human intervention.

Aim of the study. To evaluate and test the effectiveness of the upgraded QGIS plugin in tasks of automated anomaly detection from satellite data, and to apply this tool for a comprehensive geoecological assessment of riparian areas under different levels of anthropogenic pressure.

Study objectives.

• identify the most degradation-prone areas using RS observations and GIS-based methods;

• assess the geoecological state of the selected territories;

• determine the main drivers of degradation in the case study areas;

• verify the role and effectiveness of the plugin in achieving these goals.

**Methods**

***Plugin Version Differences***

The developed QGIS plugin is designed to detect anomalous deviations in raster data, i.e., areas exhibiting statistically significant divergence of indicator (index) values from the background level. Although the general user interface and workflow remain consistent with the previous version (Hudak et al., 2025; Marhes, & Hudak, 2025), the updated version incorporates substantial functional improvements. The algorithm now consists of four sequential stages:

1. plugin initialization;
2. selection of raster imagery and the relevant spectral band;
3. iterative histogram generation based on user-defined threshold values;
4. automated creation of a vector layer derived from histogram-based classification results.

The modular code structure was reorganized by dividing primary processes into dedicated functions, thereby improving readability, maintainability, and processing efficiency. Newly introduced functions include:

• *get_raster_band* – reads raster band data during each histogram update;

• *download_histogram* – exports histograms as images for detailed interpretation;

• *set_histogram_range / set_histogram_range_values* – compute and update threshold values;

• *show_histogram_in_graphicsview* – generates histograms and integrates them into the plugin interface;

• *check_threshold* – verifies and updates threshold parameters;

• *initial_update_on_first_click* – ensures threshold verification and histogram generation during first initialization;

• *raster_creation / vector_creation* – responsible for raster processing and polygonization of anomalous zones.

Together, these functions provide a robust framework for raster analysis and facilitate the reliable detection of potentially anomalous geospatial areas. The algorithm is implemented using Python libraries available within the OSGEO (Open Source Geospatial Foundation) package, which simplifies installation without requiring additional software. The plugin is officially registered in the QGIS repository under ID 4092 (Fig. 1).

***Key Improvements Compared to the Previous Version***

1. Histogram visualization and export. A new window was added for histogram display with export capability. Histograms are generated using the linspace method (NumPy) to form evenly distributed pixel intensity intervals and the plot function (matplotlib.pyplot) to produce smooth frequency distribution curves. Lower and upper thresholds are displayed separately. The QPixmap class integrates raster histogram images into the plugin interface, while saving is implemented via the getSaveFileName method of QFileDialog. This approach combines numerical analysis with interactive visualization,

improving the interpretation of remote sensing data and enhancing preprocessing quality in QGIS.

2. Spectral band selection. Unlike the previous version, which defaulted to the first band, the upgraded plugin allows users to select the required spectral range for analysis.

3. Enhanced thresholding mechanism. The threshold-selection logic was refined to allow simultaneous adjustment of both lower and upper values. Interactive input fields were added to the interface, enabling single- or dual-threshold criteria with automatic histogram updates.

4. Updated analytical parameters. The plugin interface has been expanded with modified forms and interactive components that increase its analytical flexibility and usability (Fig. 2).

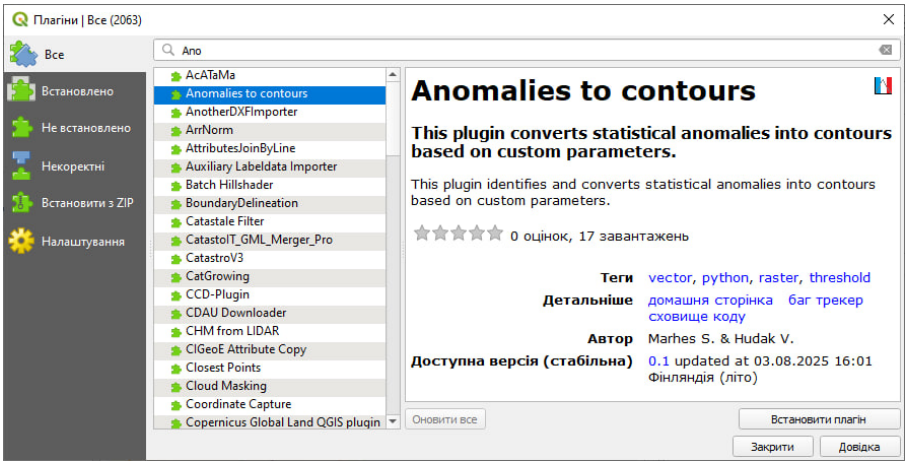


**Fig. 1. Plugin search window in the QGIS repository**

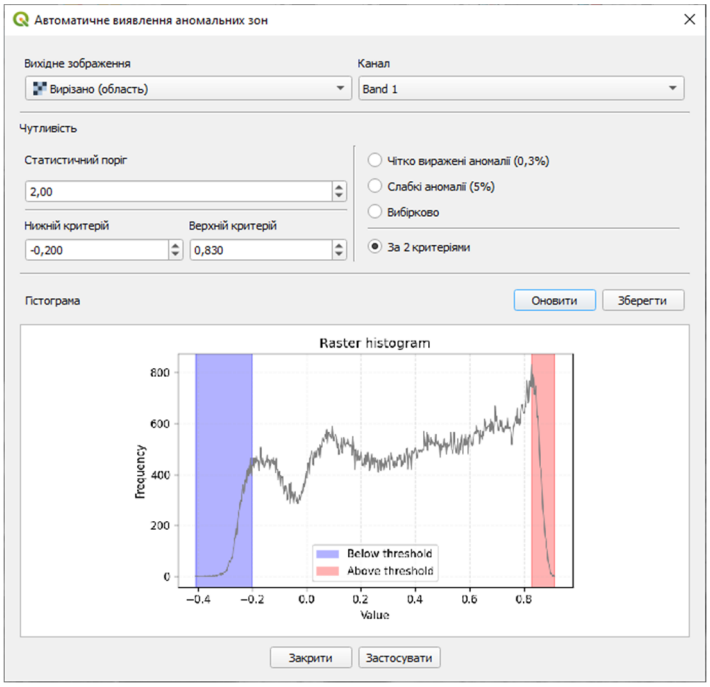


**Fig. 2. User interface of the upgraded QGIS plugin**

The improved plugin ensures rapid and accurate anomaly detection. After specifying the required parameters and generating histograms, users can apply the chosen thresholds to initiate raster and vector processing. The output is a vector layer representing the spatial distribution of anomalous zones, which can be directly integrated into further GIS-based analyses.

***Study Area***

The research focused on two contrasting riparian zones within the Dnipro River basin (Fig. 3):

- the highly urbanized banks of the Dnipro River in Kyiv;
- the riparian area of the Supii River – a left tributary of the Dnipro – within agricultural landscapes of Cherkasy and Kyiv regions.

The Dnipro River banks in Kyiv are subject to intense anthropogenic pressure (Filipovych, Lischenko, & Marhes, 2023; Ivanik et al., 2023; Streltsov, & Kril, 2025). This zone is marked by dense residential and industrial construction, extensive transportation infrastructure, and heavy recreational use. These factors drive the transformation of natural cover, soil compaction, and local degradation of riparian lands through artificial shoreline modification, expansion of impermeable surfaces, and accumulation of pollutants, particularly heavy metals (Tobias et al., 2018). Continuous anthropogenic activities, including construction and infrastructural interventions, further exacerbate soil degradation risks.

ISSN 1728-3817

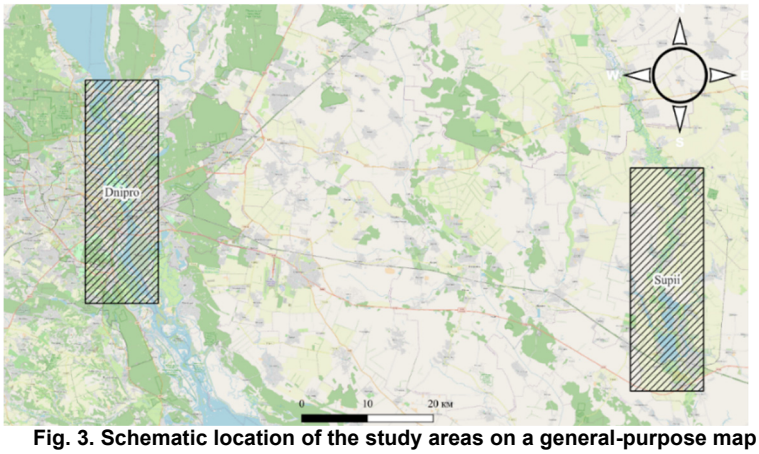


**Fig. 3. Schematic location of the study areas on a general-purpose map**

In contrast, the Supii River riparian zone is dominated by natural and agricultural landscapes. It shows minimal urbanization, limited engineering interventions, and a mosaic of croplands interspersed with patches of natural vegetation. Soils in this area are less disturbed by human activity, operating under relatively stable hydrological and ecological conditions, and demonstrating greater resilience to degradation processes (Marhes, 2024).

A comparative analysis of these two contrasting riparian sites with distinct levels of anthropogenic impact enables both the assessment of spatial variability in soil degradation and the identification of primary drivers of degradation processes. This dual-site approach provides a comprehensive understanding of the interaction between natural dynamics and anthropogenic pressures, while revealing patterns of localized anomalies within river basin systems.

***Remote Sensing Data and Preprocessing***

The study employed high-resolution satellite imagery (10–30 m), enabling detailed mapping of riparian landscapes, identification of local anomalies, and analysis of the spatiotemporal dynamics of geoecological processes (Table 1).

***Table 1***

**Characteristics of analysis periods for selected Landsat and Sentinel-2 images**

| Mission | Date | Image characteristics |
|---|---|---|
| Landsat 5 | 25/08/1985 | LANDSAT/LT05/C02/T1_L2/ LT05_181025_19850825 |
| Landsat 8 | 06/07/2025 | LANDSAT/LC08/C02/T1_L2/ LC08_181025_20250706 |
| Landsat 9 | 15/08/2025 | LANDSAT/LC09/C02/T1_L2/ LC09_181025_20250815 |
| Sentinel-2 | 10/08/2025–20/08/2025 | Mean composite for the Dnipro area with <2% cloudy pixels |
| Sentinel-2 | 10/08/2025–20/08/2025 | Mean composite for the Supii area with <2% cloudy pixels |

Landsat 5, Landsat 8, and Landsat 9 datasets were used as the primary basis for long-term monitoring. Their high spatiotemporal resolution enables tracking of multi-decadal trends in land cover transformation, water balance, and vegetation dynamics. Standardized radiometric and geometric parameters provide a reliable foundation for applying normalized indices (e.g., NDVI, NDMI, NDWI), ensuring consistent assessments across basin-scale systems.

The Landsat Collection 2, Level-2 (Surface Reflectance) products are stored as integer values and require rescaling to physically meaningful reflectance coefficients. This is achieved using a scale factor of 0.0000275 and an offset of −0.2, following the equation (European Space Agency, 2025a):

$$Reflectance = Raw\,Value \times 0.0000275 - 0.2 \quad (1)$$

Sentinel-2 data, acquired under the Copernicus program of the European Space Agency (ESA), were used as reference datasets. The Sentinel-2 system (Sentinel-2A and Sentinel-2B) offers high revisit frequency, broad spectral coverage (12 bands ranging from visible to near-infrared), and free accessibility (ESA, 2025). These features make it a powerful resource for monitoring vegetation conditions, soil dynamics, and spatiotemporal patterns of ecological processes in riparian zones.

The study employed the Harmonized Sentinel-2 MSI: Level-2A product (COPERNICUS/S2_SR_HARMONIZED), which provides atmospherically corrected surface reflectance values. Harmonized calibration between Sentinel-2A and Sentinel-2B ensures temporal consistency and comparability. Spectral data were rescaled using the following formula (European Space Agency, 2025b):

$$Reflectance = Raw\,Value \times 0.0001 \quad (2)$$

Of the 12 Sentinel-2 spectral bands, only four (B2 – Blue, 490 nm; B3 – Green, 560 nm; B4 – Red, 665 nm; B8 – Near Infrared, 842 nm) have a spatial resolution of 10 m, while the others are available at 20 or 60 m (European Union/ESA/Copernicus, n.d.). This discrepancy influences the level of spatial detail depending on the selected spectral bands.

Before data application, standard preprocessing steps were carried out:

• masking of clouds, haze, and shadows using QA60 bit masks;

• conversion of scaled integer values into surface reflectance coefficients;

• visual and geometric corrections to remove artifacts and ensure spatial consistency.

All computational procedures were performed within the Google Earth Engine (GEE) environment, which enabled efficient access to atmospherically corrected datasets, automated spectral index calculations, and streamlined classification of satellite imagery (Fig. 4).

***Data interpretation methods***

Soil degradation processes typically manifest through transformations of surface morphology, including alterations of microrelief, development of erosional forms, solonetz formation, and mass-movement phenomena. Contemporary Earth Observation (EO) technologies make it possible to

efficiently detect and assess these morphological features across extensive areas by analyzing spectral indicators of the land surface, structural modifications, and moisture-related parameters (Wang et al., 2023).

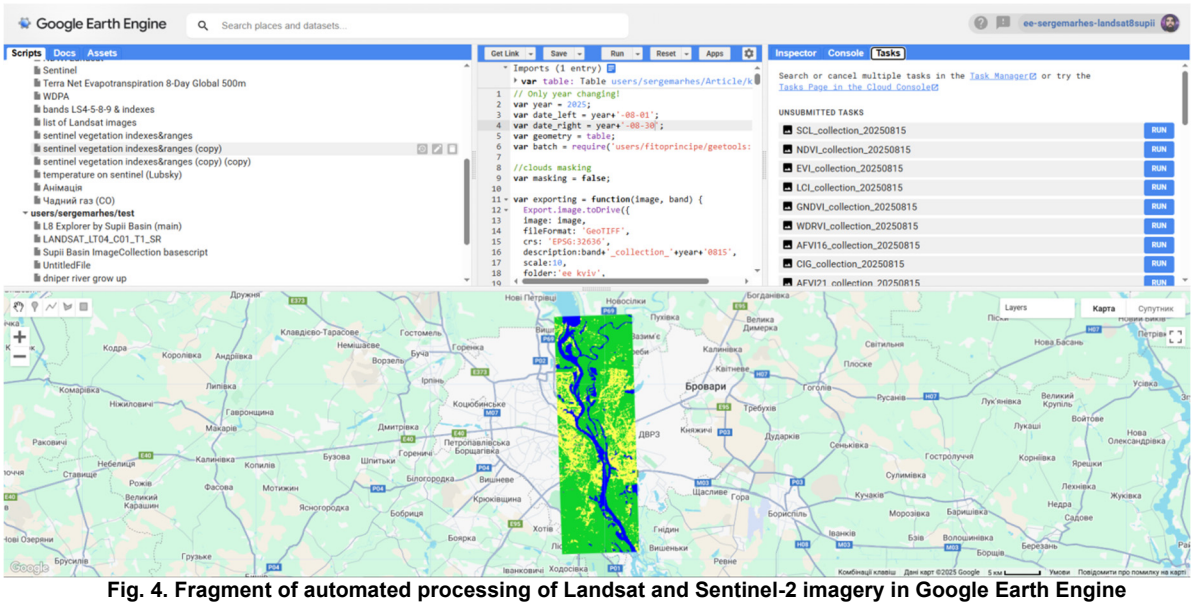


**Fig. 4. Fragment of automated processing of Landsat and Sentinel-2 imagery in Google Earth Engine**

***Principal Forms of Soil Degradation***

The major forms of soil degradation documented in global and regional studies include:

• water and wind erosion (Scholten, & Seitz, 2019);

• salinization and acidification, leading to fertility decline and humus loss (Huang et al., 2023);

• contamination by heavy metals and chemical compounds (Tóth et al., 2018);

• desertification processes, often driven by climatic and anthropogenic pressures (Chaudhuri et al., 2023).

***Spectral Indices for Spatial Analysis***

To conduct spatial diagnostics, we employed a comprehensive suite of vegetation-, water-, and soil-related indices (NDVI, GNDVI, SAVI, NDMI, NDWI, MNDWI, NDPI, NDDI, NDTI, NDSI). These indices are particularly valuable for tracing the precursors, dynamics, and manifestations of degradation processes.

Conceptually, their design is grounded in the Normalized Difference Index (NDI) framework, calculated as the normalized difference between two spectral bands. This methodological foundation, first introduced with the Normalized Difference Vegetation Index (NDVI) in 1973 (Rouse et al., 1973), allows specific biophysical and surface properties to be distinguished from multispectral observations.

***Vegetation Indices***

• *NDVI (Normalized Difference Vegetation Index)* (Rouse et al., 1973):

$$NDVI = \frac{NIR-RED}{NIR+RED}. \quad (3)$$

Higher values (> 0.5) indicate dense, healthy vegetation; low or negative values correspond to degraded vegetation or bare surfaces.

• *SAVI (Soil-Adjusted Vegetation Index)* (Huete, 1988):

$$SAVI = \frac{(1+L)(NIR-RED)}{NIR+RED+L}, \; L=0.5. \quad (4)$$

The soil-brightness correction (L) improves vegetation assessment over sparsely vegetated or bright soils.

• *GNDVI (Green Normalized Difference Vegetation Index)* (Gitelson et al., 2002):

$$GNDVI = \frac{NIR-GREEN}{NIR+GREEN}. \quad (5)$$

More sensitive than NDVI to chlorophyll content, GNDVI better reflects early physiological stress (e.g., water or nitrogen deficits).

**Water and Moisture Indices**

• *NDWI (Normalized Difference Water Index)* (McFeeters, 1996):

$$NDWI = \frac{GREEN-NIR}{GREEN+NIR}. \quad (6)$$

Enhances open-water detection due to strong NIR absorption and higher reflectance in the green band for water bodies.

• *MNDWI (Modified Normalized Difference Water Index)* (Xu, 2006):

$$MNDWI = \frac{GREEN-SWIR}{GREEN+SWIR}. \quad (7)$$

Reduces confusion among water, built-up land, and vegetation, improving delineation of small or urban water bodies.

• *NDMI (Normalized Difference Moisture Index) (Gao, 1996):*

$$NDMI = \frac{NIR-SWIR}{NIR+SWIR}. \quad (8)$$

Sensitive to vegetation and surface moisture; used for drought monitoring, crop condition assessment, wildfire impacts, and soil wetness.

• *NDPI (Normalized Difference Pond Index)* (Lacaux et al., 2007):

$$NDPI = \frac{SWIR-GREEN}{SWIR+GREEN}. \quad (9)$$

Facilitates detection of ponds, shallow waters, and wetland features within densely vegetated settings.

**Drought, Turbidity, and Salinity Indices**

• *NDDI (Normalized Difference Drought Index)* (Gu et al., 2007):

$$NDDI = \frac{NDVI - NDWI}{NDVI + NDWI}. \quad (10)$$

Positive values indicate drier conditions; negative values correspond to moist or hydrologically stable environments – useful for agromonitoring and drought-risk appraisal.

• *NDTI (Normalized Difference Turbidity Index)* (Lacaux et al., 2007):

$$NDTI = \frac{RED-GREEN}{RED + GREEN}. \quad (11)$$

Captures water turbidity, particularly under seasonal erosion, flood events, or anthropogenic inputs.

• *NDSI (Normalized Difference Salinity Index) (Bannari et al., 2008):*

$$NDSI = \frac{SWIR1 - SWIR2}{SWIR1 + SWIR2}. \quad (12)$$

Applied to diagnose soil salinity; values below 1 generally indicate non-saline conditions, whereas higher values are associated with elevated salinity.

Overall, the integration of spectral indices with multispectral Earth Observation datasets provides a solid framework for diagnosing soil degradation. By connecting morphological indicators with quantitative spectral parameters, this approach enables reliable detection of ecological changes and comprehensive evaluation of soil, vegetation, and water conditions. The methodology not only improves the accuracy of geoecological monitoring but also establishes a foundation for subsequent spatio-temporal analysis of degradation dynamics.

**Results**

***Change by Indeces***

A spatial analysis of anomalous values derived from Sentinel-2 satellite imagery was conducted. The anomalies represent statistically significant deviations from the background state of the territory and facilitate the detection of areas undergoing the most pronounced transformations, as indicated by the respective spectral indices. For each index, specific selection criteria were defined (Table 2), enabling the delineation of localized hotspots of potential degradation, evaluation of ongoing geoecological processes, and preliminary interpretation of spatial structures.

***Table 2***

**Criteria for identifying anomalous index values across test areas**

| Test area | Index | Low anomalies range from -1 | High anomalies up to 1 |
|---|---|---|---|
| Dnipro | GNDVI | -0.4 | 0.8 |
| | MNDWI | -0.7 | 0.5 |
| | NDMI | -0.25 | 0.5 |
| | NDPI | 0 | 0.7 |
| | NDSI | 0 | 0.42 |
| | NDTI | -0.35 | 0.1 |
| | NDVI | 0 | 0.85 |
| | SAVI | -0.05 | 0.6 |
| Supii | GNDVI | 0.25 | 0.85 |
| | MNDWI | -0.75 | 0 |
| | NDMI | -0.02 | 0.52 |
| | NDPI | 0.2 | 0.7 |
| | NDSI | 0 | 0.45 |
| | NDTI | -0.4 | 0.15 |
| | NDVI | 0.13 | 0.87 |
| | SAVI | 0.07 | 0.8 |

On the basis of these ranges, anomalous values were extracted, vectorized with the authors' custom QGIS plugin, and visualized cartographically (Fig. 5).

***Interpretation of Index-Based Anomalies***

The interpretation of spectral analysis results revealed consistent patterns reflecting both natural dynamics and anthropogenic transformations of landscapes. A decline in vegetation indices (NDVI, SAVI, GNDVI) was observed, clearly indicating reductions in biomass and photosynthetic activity. Such patterns are characteristic of territories subjected to strong anthropogenic pressures, including overgrazing, deforestation, agricultural expansion, or erosional processes, and may also reflect reduced ecological resilience to external stressors.

The GNDVI index proved particularly informative, given its sensitivity to chlorophyll content. Declining values indicate nitrogen and macroelement deficiencies in soils, pointing to deteriorating trophic conditions. Frequently, this serves as a marker of cropland degradation, where long-term agricultural use leads to fertility loss and heightened vulnerability to exhaustion or desertification.

Hydrological indices such as NDMI and MNDWI revealed shifts in vegetation and soil moisture regimes. Decreasing values reflected moisture deficits caused by both natural factors (climatic variability, aridization) and anthropogenic interventions (artificial drainage). These patterns are especially concerning under global climate change scenarios, where reduced soil and vegetation moisture acts as a precursor to agro-landscape degradation and heightened desertification risk.

Rising NDSI values signaled secondary salinization, characterized by the accumulation of salts in upper soil horizons. This process deteriorates soil physical and chemical properties, reduces productivity, and undermines the capacity to sustain stable vegetation cover. Simultaneously, increases in NDTI pointed to elevated water turbidity, are often associated with erosion, suspended sediment transport, or anthropogenic activities such as reclamation works and unsustainable water management.

Combined increases in NDPI and MNDWI alongside declining NDVI highlighted zones of waterlogging with suppressed vegetation cover, typical of swamps, flooded lands, or oversaturated soils. Similarly, high NDDI values in conjunction with low SAVI reflected moisture deficit and vegetation stress, characteristic of arid territories or areas affected by prolonged drought.

Finally, the simultaneous increase in NDSI and MNDWI values was interpreted as an indication of anthropogenic water pollution and chemical alterations. These effects are typically linked to technogenic pressures, agricultural runoff, or rising mineralization. Such processes have a multifaceted impact on ecological stability, underscoring the necessity of continuous monitoring within integrated geoecological assessment frameworks.

The summarized results are provided in Table 3. To adequately capture degradation dynamics, long-term temporal analysis was also undertaken.

***Dynamic Analysis***

To evaluate long-term dynamics, Landsat imagery spanning 1985–2025 was analyzed. Each index was categorized into two classes: values below 0 and values above 0. Transitions from negative to positive were interpreted as improvements, whereas the reverse was considered degradation. Areas without change were excluded from subsequent analysis.

For the Dnipro test site, manual vector corrections were applied to reduce the impact of cloud contamination. Landsat 9 imagery from 15 August 2025 served as the baseline, supplemented by Landsat 8 data from 6 July 2025 to fill cloud-affected gaps.

Figures 6 and 7 illustrate the index-based changes for the Dnipro and Supii sites, respectively.

*Table 3*

**Summary of index utility by interpretation domain**

| Research focus | Interpretation | Key indices |
|---|---|---|
| Vegetation cover | Activity and degradation of vegetation | NDVI, SAVI, GNDVI |
| Chlorophyll & nitrogen | Leaf status, photosynthetic performance | GNDVI, SAVI |
| Water bodies | Permanent and temporary water detection | MNDWI, NDMI |
| Soil moisture | Moisture availability | NDMI, NDSI |
| Drought | Areas prone to water deficit | NDDI, SAVI |
| Wetlands & ponds | Shallow or silted aquatic areas | NDPI, NDMI |
| Water turbidity | Sediment and pollution levels | NDTI, NDPI |
| Water quality (urban/agro) | Anthropogenic impacts | NDSI, MNDWI |
| Exogenous processes | Surface runoff, slope erosion, vegetation decline | NDVI, SAVI, NDDI |

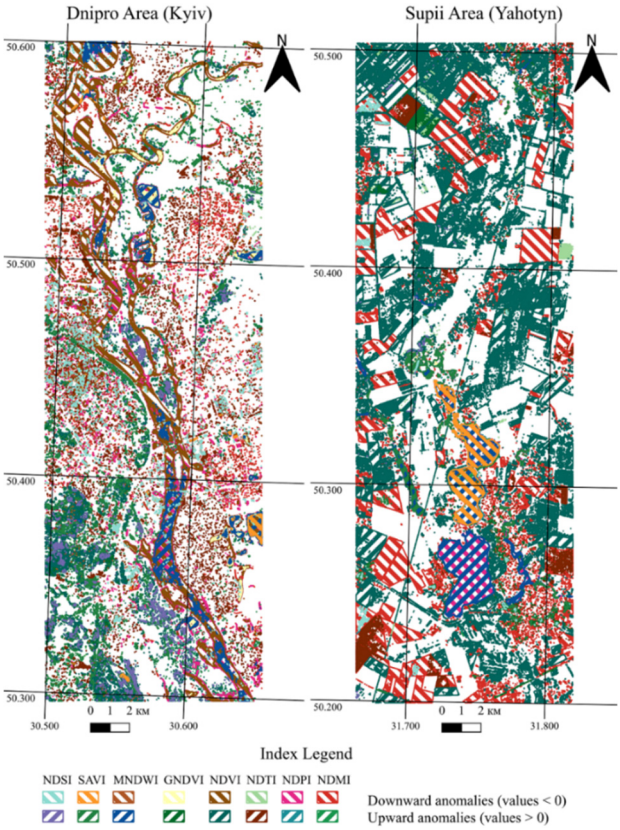


**Fig. 5. Anomalous zones in the Dnipro (left) and Supii (right) test areas, derived from Sentinel-2 index data**

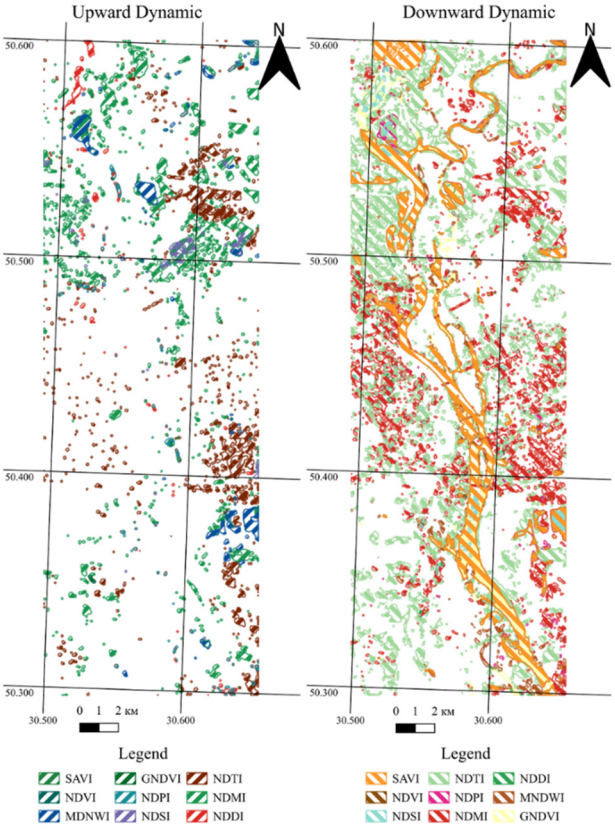


**Fig. 6. Index-based changes in the Dnipro site (Kyiv) from 1985–2025**

A set of normalized spectral indices was computed to assess different aspects of geoecological processes. Their cartographic visualization revealed spatial patterns associated with vegetation cover, soil moisture dynamics, salinization, anthropogenic pressures, and water quality. This approach facilitated not only the rapid detection of degradation phenomena but also the ability to trace their dynamics at a regional scale.

The classification of results was based on comparisons of negative and positive index ranges (Table 4). Positive values typically indicated the presence or intensity of a process (e.g., dense vegetation for NDVI, SAVI, GNDVI, or salinization for NDSI), whereas negative values corresponded to absence or opposite states (bare soils, urbanized zones, low moisture). This framework allowed for generalization at the macro level without element-by-element examination, thereby improving monitoring efficiency and enabling comparisons across areas with varying anthropogenic load.

The final stage involved synthesizing multi-index and temporal data to identify zones of active soil degradation (Fig. 8). The generalized outcomes provide a solid scientific basis for ecological monitoring, preventive measures, and adaptive strategies within urbanized watershed systems.

ISSN 1728-3817

*Table 4*

**Interpretation of spectral indices by positive and negative values**

| Index | Negative values (Downward dynamic) | Positive values (Upward dynamic) |
|---|---|---|
| **NDVI** | Bare or degraded soil, urban areas, water | Healthy, dense vegetation with high chlorophyll |
| **SAVI** | Bare or stressed soil | Healthy cover even with partial bare soil |
| **GNDVI** | Low photosynthesis, bare soil, water | High photosynthetic activity, chlorophyll-rich leaves |
| **MNDWI** | Urban or dry soils, vegetation | Open water, saturated soils |
| **NDMI** | Dry soil, water-stressed vegetation | Moist soils, healthy vegetation |
| **NDPI** | No ponds or wetlands | Shallow water, wetlands, silted ponds |
| **NDDI** | Moist conditions | Drought-prone, water-deficit areas |
| **NDTI** | Clear water, low turbidity | Turbid, polluted water |
| **NDSI** | Non-saline soils | Saline soils, secondary salt crusts |

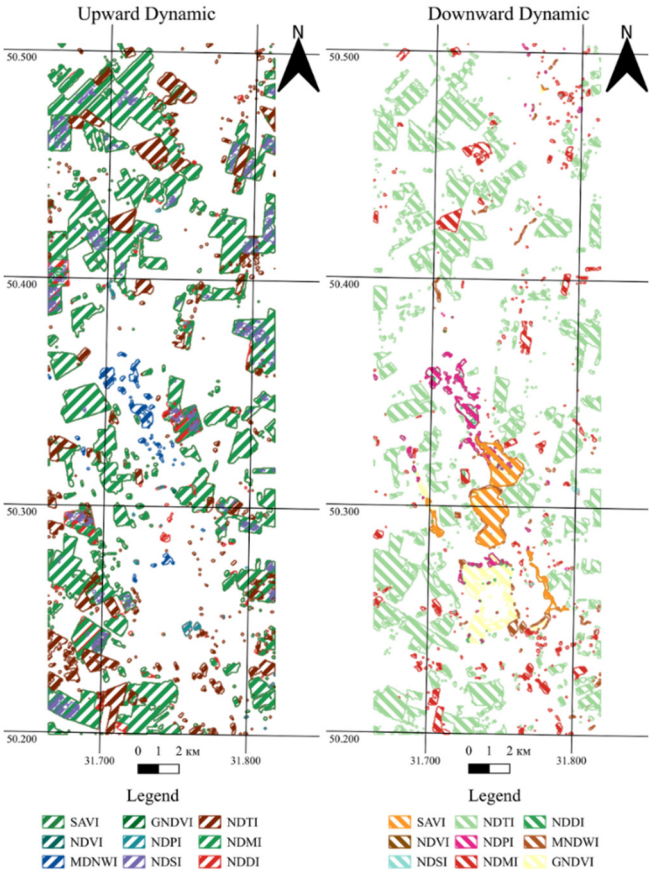


**Fig. 7. Index-based changes in the Supii site (Yahotyn) from 1985–2025**

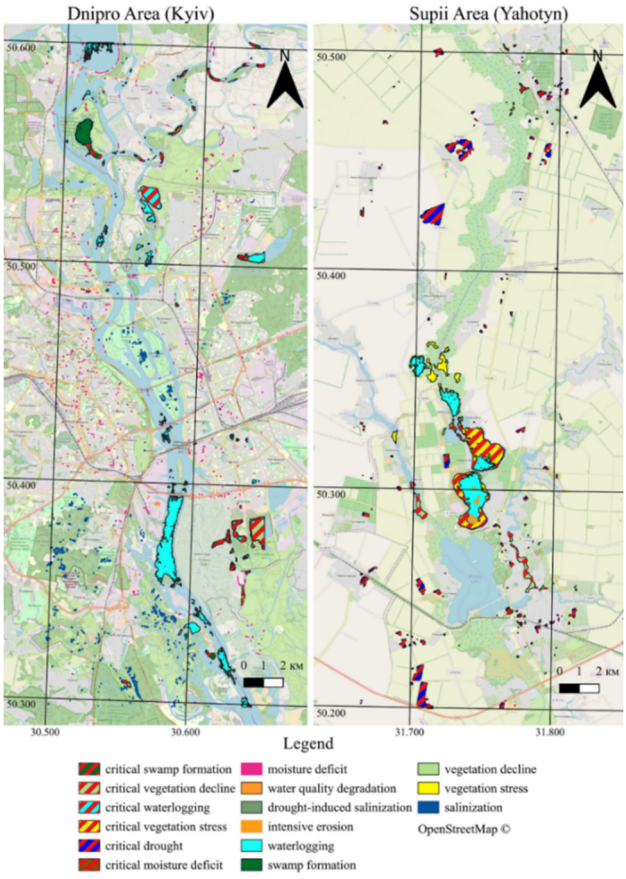


**Fig. 8. Result of index-based synthesis indicating potential forms of soil degradation**

The integration of multi-index data with four decades of temporal dynamics enabled the identification of several key forms of degradation: swamp formation, vegetation decline and stress, waterlogging, drought, moisture deficit, water quality deterioration, salinization, and intensive erosion. This comprehensive approach produced a synthetic map of degradation-prone territories, combining long-term temporal series with spatial localization of anomalies.

Specifically, in the Dnipro site, widespread waterlogging was observed downstream of the Southern Bridge; salinization was detected on Trukhaniv Island and in Holosiivskyi Forest; and in the Osokorky meadows, vegetation decline, waterlogging, and swamp formation were recorded. Across Kyiv, persistent moisture deficits were identified, frequently overlapping with densely urbanized areas. Additionally, active swamp formation was observed in the "Ptashynyi Rai" park, while vegetation degradation was evident near the mouth of the Desna River.

In the Supii site near Yahotyn, vegetation stress occurred along reservoir banks, while drought phenomena dominated the northern agricultural lands. Intensive erosion was further identified within one reservoir, particularly in areas with small islands.

Although the proposed approach demonstrates considerable potential, it remains experimental. Its reliability can be significantly enhanced through the integration of additional ecological variables, including topographic parameters (slope steepness and curvature), soil and atmospheric temperature, and evapotranspiration rates. Considering these factors, which directly affect soil moisture dynamics and surface stability, would substantially improve the accuracy of degradation assessments and support the development of more reliable cartographic representations of soil conditions.

**Discussion and conclusions**

The custom QGIS plugin developed and refined by the authors has demonstrated high efficiency in the semi-automated detection of anomalous zones based on satellite data. Its key advantage lies in the rapid transformation of complex and masked raster datasets into vector polygons,

which considerably simplifies subsequent spatial analysis and enhances the interpretability of results. The implemented improvements – such as algorithmic determination of threshold values for low and high anomalies, histogram-based data visualization, and automatic computation of statistical attributes for each polygon – have significantly expanded the functionality of the tool. These innovations have increased their practical value for geoecological research. At the same time, certain limitations were revealed, particularly in relation to processing large raster datasets, highlighting the need for further optimization of computational performance.

The application of the plugin to two contrasting test sites – the Dnipro River within the Kyiv metropolitan area and the Supii River in predominantly agricultural landscapes – enabled the integration of long-term Landsat archives (1985–2025) with contemporary Sentinel-2 imagery (2025). This integrative approach revealed spatio-temporal patterns of degradation processes, including vegetation decline, waterlogging, drought stress, salinization, and intensive erosion. The resulting maps provide clear spatial localization of risk zones and allow for the tracing of their evolution over recent decades. These outputs form a robust basis for forecasting degradation trends and for developing targeted protective and adaptive measures at the regional scale.

A generalized correspondence matrix linking spectral indices with specific forms of soil degradation was also developed. This matrix functions as a practical identification framework, enabling rapid association of index values with degradation types. For instance, high NDSI values combined with positive MNDWI indicate salinization and waterlogging, whereas decreasing NDVI alongside elevated NDDI signals vegetation stress under drought conditions. This methodological reference improves the efficiency of remote sensing data interpretation and facilitates the selection of relevant indices for targeted monitoring programs.

Future directions for the development of the plugin encompass several areas. First, the integration of machine learning algorithms could enable automated classification of degradation processes, reducing the subjectivity of interpretation. Second, the incorporation of Big Data processing and parallel computing frameworks would enhance scalability, ensuring efficient handling of extensive satellite archives. Third, the addition of auxiliary ecological variables – such as topographic parameters, soil and air temperature, or climatic indicators – would increase the precision of spatio-temporal modeling. Finally, implementation of the plugin technology with cloud-based remote sensing services, such as Google Earth Engine, would enable real-time access to updated datasets and broaden its operational applicability.

Overall, the integration of the improved semi-automated interpretation tool with multi-decadal datasets and generalized index-based classification schemes establishes a coherent methodology for monitoring soil degradation processes. The findings confirm the effectiveness of the proposed approach, although it remains experimental and requires further validation through supplementary ecological and ground-truth data.

The scientific novelty of this research lies in the integration of an enhanced automated remote sensing interpretation tool with a multi-level framework for spectral index interpretation. This synergy enables both the rapid identification of anomalous zones and a comprehensive spatio-temporal evaluation of degradation phenomena. The practical significance of the plugin lies in providing an accessible tool for local authorities, environmental agencies, and research institutions, with applications in urban monitoring, agricultural landscape management, and ecological risk forecasting. With advancements in machine learning, large-scale data processing, and cloud-based platforms for remote sensing, the plugin has strong potential to evolve into a universal instrument for systemic ecological analysis and decision support.

**Authors' contribution:** Serhii Marhes – conceptualization, data validation, methodology, writing (original draft); Vasyl Hudak – writing (review and editing), databases and data analysis, methodology; Vitaliy Zatserkovnyi – formal analysis, revising of the manuscript; Volodymyr Filipovych – formal analysis, revising of the manuscript, Mauro De Donatis – revision and editing.

**Sources of funding.** This research has been done in the framework of the project №25БП049-01(М) "Integrated models and forecasting of natural and military geohazards and assessment of their impact on critical infrastructure" and was funded by the Ministry of Education and Science of Ukraine, and of the EU Project LOC3G (grant No 101129729, MARIE SKLODOWSKA-CURIE ACTIONS (MSCA)).

**References**

Adgo, E., Teshome, A., & Mati, B. (2013). Impacts of long-term soil and water conservation on agricultural productivity: The case of Anjenie watershed, Ethiopia. *Agricultural Water Management*, 117, 55–61. https://doi.org/10.1016/j.agwat.2012.10.026

Bannari, A., Guedon, A. M., El-Harti, A., Cherkaoui, F. Z., & El-Ghmari, A. (2008). Characterization of slightly and moderately saline and sodic soils in irrigated agricultural land using simulated data of Advanced Land Imager (EO-1) sensor. *Communications in Soil Science and Plant Analysis*, 39(19–20), 2795–2811. https://doi.org/10.1080/00103620802432717

Bouza, M. E., Aranda-Rickert, A., Brizuela, M. M., et al. (2016). Economics of land degradation in Argentina. In E. Nkonya, A. Mirzabaev, & J. von Braun (Eds.), *Economics of land degradation and improvement – A global assessment for sustainable development*. Springer. https://doi.org/10.1007/978-3-319-19168-3_11

Chaudhuri, S., Roy, M., McDonald, L. M., & Emendack, Y. (2023). Land degradation–desertification in relation to farming practices in India: An overview of current practices and agro-policy perspectives. *Sustainability*, 15(8), Article 6383. https://doi.org/10.3390/su15086383

European Space Agency. (2025a). *Introducing Sentinel-2*. https://www.esa.int/Applications/Observing_the_Earth/Copernicus/Sentinel-2/Introducing_Sentinel-2

European Space Agency. (2025b). *Sentinel-2 products*. Copernicus Sentinel Wiki. https://sentiwiki.copernicus.eu/web/s2-products

European Union/ESA/Copernicus. (n.d.). *Sentinel-2 products*. Copernicus Sentinel Wiki. https://sentiwiki.copernicus.eu/web/s2-products

Filipovych, V., Lischenko, L., & Marhes, S. (2023). Methodology for assessing and forecasting the landslide hazard on the territory of the Dnieper landslide zone in the city of Kyiv based on satellite data. *Fourth EAGE Workshop on Assessment of Landslide Hazards and Impact on Communities* (pp. 1–5). European Association of Geoscientists & Engineers. https://doi.org/10.3997/2214-4609.2023500007

Filipovych, V., Lischenko, L., & Marhes, S. (2025). Monitoring of activation and neotectonic dependence of landslide processes within the Right Bank of Kyiv. *Fifth EAGE Workshop on Assessment of Landslide Hazards and Impact on Communities* (pp. 1–5). European Association of Geoscientists & Engineers.

Gao, B.-C. (1996). NDWI–A normalized difference water index for remote sensing of vegetation liquid water from space. *Remote Sensing of Environment*, 58(3), 257–266. https://doi.org/10.1016/S0034-4257(96)00067-3

Gitelson, A. A., Kaufman, Y. J., Stark, R., & Rundquist, D. (2002). Novel algorithms for remote estimation of vegetation fraction. *Remote Sensing of Environment*, 80, 76–87. https://doi.org/10.1016/S0034-4257(01)00289-9

Gu, Y., Brown, J. F., Verdin, J. P., & Wardlow, B. (2007). A five-year analysis of MODIS NDVI and NDWI for grassland drought assessment over the central Great Plains of the United States. *Geophysical Research Letters*, 34(6). https://doi.org/10.1029/2006GL029127

Higginbottom, T. P., & Symeonakis, E. (2014). Assessing land degradation and desertification using vegetation index data: Current frameworks and future directions. *Remote Sensing*, 6(10), 9552–9575. https://doi.org/10.3390/rs6109552

Huang, K., Li, M., Li, R., Rasul, F., Shahzad, S., Wu, C., Shao, J., Huang, G., Li, R., Almari, S., Hashem, M., & Aamer, M. (2023). Soil acidification and salinity: The importance of biochar application to agricultural soils. *Frontiers in Plant Science*, 14, Article 1206820. https://doi.org/10.3389/fpls.2023.1206820

Hudak, V., Kril, T., & Zatserkovnyi, V. (2025). Remote monitoring of vertical surface displacements as indicators of deformation of underground structures. *Visnyk of Taras Shevchenko National University of Kyiv. Geology*, 1(108), 94–102. https://doi.org/10.17721/1728-2713.108.13

Hudak, V., Marhes, S., Zatserkovnyi, V., & De Donatis, M. (2025). Methodology for the automated detection of anomalous geospatial zones in satellite imagery using statistical analysis and a custom QGIS plugin. *Visnyk of Taras Shevchenko National University of Kyiv. Geology*, 3(110), 5–14.

Huete, A. R. (1988). A soil-adjusted vegetation index (SAVI). *Remote Sensing of Environment*, 25(3), 295–309. https://doi.org/10.1016/0034-4257(88)90106-X

Ivanik, O., Fonseca, J., Shabatura, O., Khomenko, R., Hadiatska, K., & Kravchenko, D. (2022). An integrated approach for landslide hazard assessment: A case study of the Middle Dnieper Basin, Ukraine. *Journal of Water and Land Development*, 52, 81–86. https://doi.org/10.24425/jwld.2021.139947

Ivanik, O., Hadiatska, K., Bondar, K., Kravchenko, D., & Tustanovska, L. (2023). Local forecasting of landslide hazard within the sites of historical and cultural heritage in Kyiv, Ukraine. *Conference Proceedings, 84th EAGE Annual Conference & Exhibition, Jun 2023* (pp. 1–5). https://doi.org/10.3997/2214-4609.202310285

Keesstra, S. D., Bouma, J., Wallinga, J., Tittonell, P., Smith, P., Cerdà, A., Montanarella, L., Quinton, J. N., Pachepsky, Y., van der Putten, W. H., Bardgett, R. D., Moolenaar, S., Mol, G., Jansen, B., & Fresco, L. O. (2016). The significance of soils and soil science towards realization of the United Nations Sustainable Development Goals. *SOIL*, 2(2), 111–128. https://doi.org/10.5194/soil-2-111-2016

Korohoda, N. P., Kovtoniuk, O. V., & Halahan, O. O. (2023). Kyiv green areas: Assessment of the functioning efficiency and volumes of ecosystem services for erosion control. *Journal of Geology, Geography and Geoecology*, 3, 516–524. https://doi.org/10.15421/112346

Kravchenko, K. O. (2023). On the study of geoecological problems of urbanization processes in the context of the Sustainable Development Concept. *Liudyna ta dovkillia. Problemy neoekolohii – Man and Environment. Problems of Neoecology*, 38, 6–19 (2022) [in Ukrainian]. [Кравченко, К. О. (2022). До питання про дослідження геоекологічних проблем урбанізаційних процесів у контексті Концепції сталого розвитку. *Людина та довкілля. Проблеми неоекології*, 38, 6–19]. https://doi.org/10.26565/1992-4224-2022-38-01

Kril, T., Cherevko, I., & Shekhunova, S. (2024). A ranking analysis of geological and engineering factors of historical monuments' stability response: A case study of Kyiv-Pechersk Lavra, Ukraine. *Buildings*, 14(10), Article 3152. https://doi.org/10.3390/buildings14103152

Kruglov, O., Hudak, V., & Kruhlov, B. (2025). Exploring D-InSAR technology for monitoring soil erosion: Case study in Kharkiv region. In *18th International Conference Monitoring of Geological Processes and Ecological Condition of the Environment* (Vol. 2025, No.1, pp. 1–5). European Association of Geoscientists & Engineers. https://doi.org/10.3997/2214-4609.2025510037

Lacaux, J.-P., Tourre, Y. M., Vignolles, C., Ndione, J. A., & Lafaye, M. (2007). Classification of ponds from high-spatial-resolution remote sensing: Application to Rift Valley Fever epidemics in Senegal. *Remote Sensing of Environment*, 106(1), 66–74. https://doi.org/10.1016/j.rse.2006.07.012

Li, R., Zhu, G., Lu, S., Sang, L., Meng, G., Chen, L., Jiao, Y., & Wang, Q. (2023). Effects of urbanization on the water cycle in the Shiyang River basin: Based on a stable isotope method. *Hydrology and Earth System Sciences*, 27, 4437–4452. https://doi.org/10.5194/hess-27-4437-2023

Marhes, S. (2024). Satellite geoecological analysis of the peat-swamp system of the Supii River. In *Ideas and Innovations in Earth – IIES (materials of the 10th International Geosciences Conference of Young Researchers, Kyiv, 23–24 May 2024)*. National Academy of Sciences of Ukraine. https://doi.org/10.30836/igs.iies.2024.34

Marhes, S., & Hudak, V. (2025). *Anomalies2Contours: QGIS plugin for anomaly detection* (Version 2.0) [Computer software]. GitHub. https://github.com/rnrhs/anomalies2contours

McFeeters, S. K. (1996). The use of the Normalized Difference Water Index (NDWI) in the delineation of open water features. *International Journal of Remote Sensing*, 17(7), 1425–1432. https://doi.org/10.1080/01431169608948714

Menshov, O., & Kruglov, O. (2023). Agricultural soil degradation in Ukraine. In P. Pereira, M. Muñoz-Rojas, I. Bogunovic, & W. Zhao (Eds.), *Impact of agriculture on soil degradation II* (pp. 325–347). Springer. https://doi.org/10.1007/698_2022_951

Nath, A., Koley, B., Choudhury, T., Saraswati, S., Ray, B. C., Um, J.-S., & Sharma, A. (2023). Assessing coastal land-use and land-cover change dynamics using geospatial techniques. *Sustainability*, 15(9), Article 7398. https://doi.org/10.3390/su15097398

Rouse, J. W., Jr., Haas, R. H., Schell, J. A., & Deering, D. W. (1973). Monitoring vegetation systems in the Great Plains with ERTS. In *Third ERTS Symposium* (pp. 309–317). NASA SP-351.

Scholten, T., & Seitz, S. (2019). Soil erosion and land degradation. *Soil Systems*, *3*(4), Article 68. https://doi.org/10.3390/soilsystems3040068

Shekhunova, S., & Kril, T. (2022). Geological and economic risk assessment for territories of hazardous geological and technogenic processes (exemplified by Solotvyno township). *Naukovyi Visnyk Natsionalnoho Hirnychoho Universytetu*, 2, 079–085. https://doi.org/10.33271/nvngu/2022-2/079

Streltsov, A., & Kril, T. (2025). Weakness zones on a slope within a landslide-prone area: A case study of the Mykilska Brama site, Kyiv. *XVIII International Scientific Conference "Monitoring of Geological Processes and Ecological Condition of the Environment"* (pp. 1–5). https://doi.org/10.3997/2214-4609.2025510071

Tobias, S., Conen, F., Duss, A., Wenzel, L. M., Buser, C., & Alewell, C. (2018). Soil sealing and unsealing: State of the art and examples. *Land Degradation & Development*, 29(6), 2015–2024. https://doi.org/10.1002/ldr.2919

Tóth, G., Hermann, T., da Silva, M. R., & Montanarella, L. (2018). Monitoring soil for sustainable development and land degradation neutrality. *Environmental Monitoring and Assessment*, 190, Article 57. https://doi.org/10.1007/s10661-017-6415-3

Wang, J., Zhen, J., Hu, W., Chen, S., Lizaga, I., Zeraatpisheh, M., et al. (2023). Remote sensing of soil degradation: Progress and perspective. *International Soil and Water Conservation Research*, 11(3), 429–454. https://doi.org/10.1016/j.iswcr.2023.03.002

Xie, R., Xiao, H., & Ashraf, M. A. (2020). Application of GIS/RS for monitoring of the ecological environment in a coastal zone. *Arab Journal of Geosciences*, 13, Article 271. https://doi.org/10.1007/s12517-020-5114-5

Xu, H. (2006). Modification of normalized difference water index (NDWI) to enhance open water features in remotely sensed imagery. *International Journal of Remote Sensing*, *27*(14), 3025–3033. https://doi.org/10.1080/01431160600589179

Yirdaw, E., Tigabu, M., & Monge, A. (2017). Rehabilitation of degraded dryland ecosystems – review. *Silva Fennica*, 51(1), Article 1673. https://doi.org/10.14214/sf.1673

**Отримано редакцією журналу / Received: 19.12.25**
**Прорецензовано / Revised: 14.01.26**
**Схвалено до друку / Accepted: 18.02.26**
**Опубліковано / Published: 27.02.26**

**Сергій МАРГЕС[1], асп.**
**ORCID ID: 0009-0004-2942-9406**
**e-mail: sergemarhes@gmail.com**

**Василь ГУДАК[2], асп.**
**ORCID ID: 0009-0002-7333-0409**
**e-mail: gudak_vasyl@knu.ua**

**Віталій ЗАЦЕРКОВНИЙ[2], д-р техн. наук, проф.**
**ORCID ID: 0009-0003-5187-6125**
**e-mail: vitalii.zatserkovnyi@knu.ua**

**Володимир ФІЛІПОВИЧ[1], канд. геол. наук, ст. наук. співроб.**
**ORCID ID: 0000-0002-9404-8122**
**e-mail: vefilin2000@gmail.com**

**Мауро ДЕ ДОНАТІС[3], канд. геол. наук, доц.**
**ORCID ID: 0000-0002-9721-1095**
**e-mail: mauro.dedonatis@uniurb.it**

**[1]Державна установа "Науковий центр аерокосмічних досліджень Землі Інституту геологічних наук Національної академії наук України", Київ, Україна**
**[2]Київський національний університет імені Тараса Шевченка, Київ, Україна**
**[3]Університет Урбіно Карло Бо, Урбіно, Італія**

# ВИЯВЛЕННЯ ПРОЦЕСІВ ДЕГРАДАЦІЇ ҐРУНТІВ У РІЧКОВИХ БАСЕЙНАХ ІЗ ВИКОРИСТАННЯМ СУПУТНИКОВИХ ІНДЕКСІВ ТА АВТОРСЬКОГО ПЛАГІНА ДЛЯ QGIS

**В с т у п .** ***У дослідженні розглядається проблема ідентифікації та оцінювання ризиків деградації ґрунтів у річкових басейнах, які суттєво впливають на екологічний стан територій. Особливу увагу приділено підвищенню ефективності просторового аналізу шляхом використання вдосконаленого плагіна для QGIS, розробленого авторами.***

**М е т о д и .** ***Програмний інструмент створено на основі пакета OSGeo для Python та інтегровано з алгоритмами зваженого накладання й напівавтоматичної векторизації результатів. Його реалізовано як внутрішній набір функцій, що не потребує додаткових встановлень. Функціонал охоплює обробку супутникових даних, автоматичне виявлення аномальних зон та побудову узагальнювальної таблиці відповідності спектральних індексів різним формам деградації. Для аналізу використано багаторічні ряди знімків Landsat (1985–2025 рр.) та дані Sentinel-2 (2025 р.), оброблені в середовищі QGIS. Тестування проведено на прикладі басейнів річок Дніпро та Супій, що відрізняються рівнем антропогенного навантаження.***

**Р е з у л ь т а т и .** ***Аналіз дав змогу виокремити закономірності деградаційних процесів, зокрема зменшення площі рослинного покриву, засолення, заболочення, прояви посух та розвиток ерозійних форм. Застосування узагальнювальної таблиці спектральних індексів оптимізувало інтерпретацію супутникових знімків і підвищило точність класифікації форм деградації. Плагін підтвердив свою ефективність у поєднанні індексного аналізу з просторовим моделюванням для оцінювання стану басейнових систем.***

**В и с н о в к и .** ***Вдосконалений інструмент довів практичну придатність для моніторингу екологічного стану територій і підтримки управлінських рішень. Наукова новизна полягає в інтеграції напівавтоматизованого дешифрування супутникових даних із багаторівневою методикою інтерпретації спектральних індексів, що забезпечує оперативне виявлення аномальних ділянок і комплексну просторово-часову оцінку деградаційних процесів. Перспективи розвитку включають інтеграцію алгоритмів машинного навчання для автоматичної класифікації процесів, застосування обробки великих масивів супутникових даних із використанням паралельних обчислень, а також інтеграцію з хмарними платформами дистанційного зондування (зокрема, Google Earth Engine) для доступу до актуальних даних у режимі реального часу. Сукупність цих рішень формує підґрунтя для створення універсальної системи прогнозування та запобігання деградаційним процесам у річкових басейнах.***

**К л ю ч о в і  с л о в а :** ***ГІС, моніторинг, екзогенні геологічні процеси, деградація ґрунтів, супутникові знімки, автоматизоване виявлення, геопросторові зони, плагін QGIS, супутникові зображення, геодинамічні аномалії, просторовий аналіз.***

Віталій Зацерковний є членом редколегії видання, тому не брав участі у рецензуванні та прийнятті рішення щодо публікації цієї статті.

Автори заявляють про відсутність конфлікту інтересів. Спонсори не брали участі в розробленні дослідження; у зборі, аналізі чи інтерпретації даних; у написанні рукопису; в рішенні про публікацію результатів.

Vitaliy Zatserkovnyi is the a member of the journal editorial board, therefore did not take part in the peer-review process or in the decision to publish of this article.

The authors declare no conflicts of interest. The funders had no role in the design of the study; in the collection, analyses or interpretation of data; in the writing of the manuscript; in the decision to publish the results.